Environmental Modelling & Software 89 (2017) 131–143

Contents lists available at ScienceDirect

Environmental Modelling & Software

journal homepage: www.elsevier.com/locate/envsoft

Development of a nitrous oxide routine for the SWAT model to assess greenhouse gas emissions from agroecosystems

Moges B. Wagena, Emily M. Bock, Andrew R. Sommerlot, Daniel R. Fuka, Zachary M. Easton*

Department of Biological Systems Engineering, Virginia Tech, Blacksburg, VA, USA

ARTICLE INFO

Article history:
Received 7 April 2016
Received in revised form
9 November 2016
Accepted 10 November 2016
Available online 29 December 2016

Keywords:
Greenhouse gas emissions
SWAT
Nitrous oxide
pH
Denitrification
Nitrification
Soil carbon
Spatial distribution

ABSTRACT

Greenhouse gas (GHG) emissions from agroecosystems, particularly nitrous oxide (N_2O), are an increasing concern. To quantify N_2O emissions from agroecosystems, which occur as a result of nitrogen (N) cycling, a new physically-based routine was developed for the Soil and Water Assessment Tool (SWAT) model to predict N_2O flux during denitrification and an existing nitrification routine was modified to capture N_2O flux during this process. The new routines predict N_2O emissions by coupling the carbon (C) and N cycles with soil moisture/temperature and pH in SWAT. The model uses reduction functions to predict total denitrification (N_2+ N_2O) and partitions N_2 from N_2O using a ratio method. The modified SWAT nitrification routine likewise predicts N_2O emissions using reduction functions. The new denitrification routine and modified nitrification routine were tested using GRACEnet data at University Park, Pennsylvania, and West Lafayette, Indiana. Results showed strong correlations between plot measurements of N_2O flux and the model predictions for both test sites and suggest that N_2O emissions are particularly sensitive to soil pH and soil N, and moderately sensitive to soil temperature/moisture and total soil C levels.

Software availability

Model name: SWAT-GHG model
Developed by: M.B. Wagena (bwmoges4@vt.edu) and Z.M. Easton (zeaston@vt.edu), Department of Biological Systems Engineering, Virginia Tech, Blacksburg, VA 24060
Year available: 2016
Availability: Contact developers
Cost: Free and open source
Language: Fortran

1. Introduction

Greenhouse gas (GHG) emissions from agroecosystems, particularly nitrous oxide (N_2O), are of increasing importance and a major contributor to global climate change. N_2O is a potent GHG, with 310 times the radiative forcing as CO_2 (Beheydt et al., 2008; Jahangir et al., 2013) and is an intermediate product produced during both denitrification (Jahangir et al., 2013) and nitrification (Parton et al., 2001). Denitrification is the microbial process that converts reactive nitrate (NO_3^-) to N_2O and unreactive dinitrogen (N_2), and is favored by anaerobic soil conditions, adequate soil NO_3^- and carbon (C) content, moderate to high soil temperature, neutral to basic soil pH, and the presence of denitrifying microorganisms (Knowles, 1982; Parton et al., 1996). Nitrification is a microbial process that transforms ammonium (NH_4^+) to NO_3^- and occurs under aerobic soil conditions in the presence of adequate NH_4^+, high soil temperature, and high pH. These factors vary in space and time in agroecosystems and interact with each other in complicated ways (Henault & Germon, 2000). Consequently, N_2O emissions vary spatially across a landscape and temporarily over the course of a year (Groffman et al., 2009). Identifying when, where, and how these factors interact to form hotspots/hot moments of N_2O emissions (e.g., areas or times of large emissions) is a current area of research and a daunting challenge. Thus, there is a need to develop integrated models capable of incorporating these relevant controls to predict N_2O emission across a range of scales to better inform the selection of landscape management practices to reduce N_2O emissions (Bruland et al., 2006; Clement et al., 2002; Mosier et al., 2002).

* Corresponding author.
E-mail address: zeaston@vt.edu (Z.M. Easton).

http://dx.doi.org/10.1016/j.envsoft.2016.11.013
1364-8152/

Numerous system dynamics models (Kelly et al., 2013) have been developed to predict N_2O emissions. Most, however, were developed for more natural systems in the absence of anthropogenic N application, where the N and C cycles are more closely coupled and N is often limiting. Consequently, the need for new models that capture N_2O emissions in landscapes with an abundance of bioavailable N is driven by the inability of models developed for natural systems without N enrichment to capture N_2O emissions when the N and C cycles are decoupled as a result of this enrichment. Existing models widely vary in their concept and structure, with some empirically-based and some process-based, and range in scale from plot to global. Generally, N_2O emission models can be classified based on their application (Shaffer, 2002): (1) relatively simple index or screening type models, (e.g. Intergovernmental Panel on Climate Change (IPPC) Tier 2 model), (2) empirically-based models, and (3) process-based models.

Empirical models rely on easily measurable parameters (e.g., soil moisture/temperature, pH, and soil nutrients) and then use regression equations to relate them to N_2O emissions (Heinen, 2006; Parton et al., 1996). Empirical models include WNMM (Li et al., 2007), NLEAP (Shaffer et al., 1991), EPIC (Williams, 1990), DLEM (Tian et al., 2015), EXPERT-N (Priesack et al., 2001), and NEMIS (Henault & Germon, 2000). While these models are capable of predicting N_2O emissions under relatively controlled and known conditions, these models can be challenging to apply outside of the range of conditions for which they were developed and thus have limited utility to drive landscape management or predict the effects of processes such as climate change.

Most of the recent advances in N_2O emission models have been made in process-based modeling, which can generally be classified in to three model types (Parton et al., 1996): (1) microbial growth models, (2) soil structure models, and (3) physically-based models.

Microbial growth models simulate N_2O emissions by representing the dynamics of the microbial community (Heinen, 2006; Parton et al., 1996). Examples of such models include the DENLEFWAT model (Leffelaar, 1988; Leffelaar & Wessel, 1988), DNDC model (Frolking et al., 1992; Li et al., 1997), NLOSS model (Riley & Matson, 2000), ECOSYS model (Metivier et al., 2009), and the RZWQM model (Shaffer et al., 2001). Factors that affect the microbial growth rate in these models are the soil N and C content, soil temperature, soil pH, and soil moisture content. Microbial growth rates are assumed to be an estimate of the N_2O emission potential of a system, that is, higher microbial growth rates translate to higher N_2O emissions. The strength of these models is the explicit representation of microbial growth and activity in the model. This includes the number and type of microbes, the community structure and the death and growth of microbes over time.

Soil structural models are based on soil physics and primarily consider the diffusion of gases and solutes into and out of soil aggregates; these models use diffusion of gases and solutes as a proxy for the anaerobic state, a primary control on N_2O emissions (Heinen, 2006; Parton et al., 1996). N_2O and nutrients such as NO_3^- and oxygen (O_2) are modeled moving into and out of soil aggregates. Soil structural models include: the Steady State Denitrification model (Arah & Smith, 1989), which predicts steady state denitrification rates as a function of soil moisture characteristics, aggregate soil particle size, oxygen reduction potential, and NO_3^- concentration; the SLIM solute leaching model (Vinten et al., 1996), which simulates N_2O emissions by considering the interaction between soil aggregates, soil moisture and O_2 diffusion; and methods described by Grant (1991), which uses a Michaelis-Menten function to predict emissions based on the soil NO_3^- concentration. The strength of soil structural models is that the anaerobic and aerobic condition of soil can be determined, resulting in the identification of denitrification and nitrification stages and hotspots in a soil. These models are well suited to assessing fine scale N_2O emissions (pore to plot scale), but require well-defined input data and/or calibration.

Physically-based, or integrated models, incorporate the relevant physical controls on N_2O emissions by simulating interactions between plant, soil, hydrologic, management, and atmospheric factors to estimate N_2O emissions. Kragt et al. (2011) and Kelly et al. (2013) suggest that integrated modeling (or integrated models) improve information transfer and decision-making by providing the ability to capture complex biological, chemical, and physical processes. Several of these integrated models exist, for example the DAYCENT (Del Grosso et al., 2002; Parton et al., 1998), DAISY (Hansen et al., 1991) and RZWQM2 models (Fang et al., 2015). These models incorporate soil parameters such as soil pH, soil temperature, soil moisture, and nutrients as driving forces controlling emissions. These models can be applied at fine or large scales with time steps of hourly to yearly and hotspots/hot moments on the landscape can be determined using these models. This class of models is generally considered the most robust and can be used outside of the range for which they were developed, unlike empirical models. This makes them ideally suited for various scenario analyses, such as assessing the impact of climate or land use change. Unfortunately, these models also require large amounts of data, some of which can be difficult to find.

In order to provide the ability to predict N_2O emissions, we developed a new physically-based routine for the Soil and Water Assessment Tool model (SWAT), hereafter referred to as SWAT-GHG. Semi-distributed, process-based models such as SWAT offer a promising platform on which to build GHG emission models because of detailed plant/crop and nutrient routines, relatively flexible hydrologic underpinnings and open source code. Indeed, recent coupling of SWAT with the biogeochemical model DAYCENT highlights the flexibility of SWAT (Wu et al., 2016). In addition, most of the parameters required to predict N_2O emissions already exist in SWAT (total soil C and N, pH, temperature and precipitation), and SWAT has built in databases for plant and soil factors, so general model initialization requires very little additional data. The development of SWAT-GHG involved a two-part addition to SWAT: first, a set of reduction functions was developed to model the total denitrification (N_2+ N_2O) and nitrification rates and second, a ratio method was applied to partition denitrification products N_2 and N_2O. The new N_2O routine was tested using plot data from the GRACEnet database in two locations: University Park, Pennsylvania, and West Lafayette, Indiana. A sensitivity analysis of total soil C and pH, N application, and climate forcing (temperature and precipitation) was performed to assess the sensitivity of the model to changes in input parameter values. We compared the predicted spatial distribution of N_2O emission at the two sites with the field level measurements to assess the ability of SWAT-GHG to elucidate where and when hotspots of N_2O production occur across agroecosystems.

2. Materials and methods

2.1. Model development

Here we describe the development of a new sub-model for SWAT, termed SWAT-GHG, to predict N_2O emissions from agroecosystems. SWAT-GHG was developed by defining a set of reduction functions based on soil and environmental factors. The soil conditions include nutrient content (NO_3^-, NH_4^+ and total soil C) and soil pH, while the environmental factors (precipitation and temperature) control the soil temperature and soil moisture conditions (Heinen, 2006; Morse et al., 2012; Weier et al., 1993). The reduction functions are based on work from Weier et al. (1993) and

Parton et al. (2001) with adjustments made for the impact of soil pH and soil temperature.

2.2. SWAT model description

The SWAT model is a process-based, semi-distributed watershed model developed to predict the impact of land management on water availability and water quality (Arnold et al., 1998). SWAT requires weather, soil, land cover, and land management data to simulate surface and subsurface hydrology and various chemical, nutrient, and sediment fluxes. SWAT-VSA re-conceptualizes SWAT to account for areas of the landscape subject to variable saturation dynamics (Easton et al., 2008). In SWTA-VSA the area of each hydrologic response unit (HRU) is defined by the coincidence of land use and wetness index class determined from a Topographic Index (TI) to differentiate areas of the landscape with respect to their moisture storage and saturation index (Easton et al., 2008). SWAT-VSA has been shown to provide better predictions of soil moisture and runoff generation than the standard SWAT model in watersheds with similar physical characteristics and climate to the study watersheds (Easton et al., 2008), and thus should provide a better platform to predict the spatial and temporal evolution of N_2O emission hotspots.

SWAT was selected as the model to build on for several reasons: it is well documented, it is supported and available as open-source code, it has robust crop/plant simulation abilities, it contains numerous potential code linkage points, and recent improvements capture the spatial and temporal evolution of saturated areas of the landscape, which are known N_2O emission hotspots (Groffman et al., 2009). Denitrification and nitrification processes are currently modeled in SWAT with first order reaction constants (e.g., denitrification only occurs above a threshold soil moisture content input by the user), but SWAT does not model N_2O emissions from either process, predicting N_2 as the only denitrification product. We incorporated the ability to predict N_2O emissions by coupling the C and N cycles with soil moisture, pH, and soil temperature by developing a denitrification subroutine "ndent_V2.f" and by modifying the existing nitrification and volatilization subroutine "nitvol.f" in SWAT. All of the parameters required to develop the routines [soil temperature, pH, and nutrient content (NH_4^+, NO_3^-, C)] are already incorporated in SWAT in various subroutines. Both subroutines predict N_2O emission at the hydrologic HRU level (the smallest unit at which the model provides output and represents a unique combination land use and moisture index).

2.2.1. Nitrous oxide model development

N_2O from denitrification was obtained by a two-part addition: (1) developing a set of equations to model the total denitrification rate (N_2+ N_2O) and (2) partitioning N_2 from N_2O. N_2O from nitrification was obtained by modifying the existing nitrification rate equation in SWAT and partitioning N_2O from NO_3.

The total denitrification flux from Parton et al. (1996) and Mosier et al. (2002) is:

$$D_{Ntotal} = \min[Fd(NO_3), Fd(C)] * Fd(\theta) * Fd(T) * Fd(pH) \quad (1)$$

where D_{Ntotal} is the denitrification rate per unit area (production of N_2 + N_2O, g N ha^{-1} d^{-1}); $Fd(NO_3)$ is the maximum total N gas flux per unit area for a given soil NO_3^- level in g N ha^{-1} d^{-1} (assuming total soil C is not limiting); Fd(C) is the maximum total N gas flux per unit area for a given total soil C level in g N ha^{-1} d^{-1} (assuming soil N is not limiting); and Fd(θ), Fd(T), and Fd(pH) are functions that represent the effects of soil moisture, soil temperature, and pH on N gas flux, respectively. While the functional form of these relationships can differ to some extent, Parton et al. (1996) and Weier et al. (1993) have developed relatively robust functions for estimating $Fd(NO_3)$, Fd(C), and Fd(θ):

$$Fd(NO_3) = 11,000 + \frac{40,000 + \text{atan}(\pi * 0.002 * (NO_3 - 180))}{\pi} \quad (2)$$

$$Fd(C) = \frac{24,000}{1 + \frac{200}{e^{0.35 * C}}} - 100 \quad (3)$$

$$Fd(\theta) = \frac{a}{b^{b^{(d * \theta)}}} \quad (4)$$

where $Fd(NO_3)$ and Fd(C) have units of g N ha^{-1} d^{-1}, θ is water-filled pore space in units of m^3 m^{-3}, C is the C content in g N ha^{-1} d^{-1}, and a, b, c and d are soil-specific fitting parameters (Table 1) to incorporate the effect of soil texture.

The soil temperature effect function, Fd(T), was derived from Seligman and Keulenv (1981):

$$Fd(T) = Max\left[\left(0.9 * \frac{Soil\ \ Temp}{Soil\ \ Temp + \exp(9.93 - 0.312 * Soil\ \ Temp)} + 0.1\right), 0.1\right] \quad (5)$$

The pH function, Fd(pH), was developed from Simek and Cooper (2002):

$$Fd(pH) = \begin{cases} 0.001 & for\ \ pH \leq 3.5 \\ \frac{pH - 3.5}{3} & for\ \ 3.5 < pH < 6.5 \\ 1 & for\ \ pH \geq 6.5 \end{cases} \quad (6)$$

We developed a ratio method to differentiate the N_2O from N_2 produced during denitrification:

$$R_{N_2/N_2O} = \min[Fr(NO_3), Fr(C)] * Fr(\theta) * Fr(pH) \quad (7)$$

where $R_{N2/N2O}$ is ratio of N_2 to N_2O, and $Fr(NO_3)$, Fr (C), Fr(θ) and Fr (pH) represent the effects of soil NO_3^--N, total soil C, soil moisture, and pH on the ratio of N_2 to N_2O, respectively. Note here that temperature is not included in the ratio prediction as increasing temperature increases both N_2 and N_2O production similarly (Parton et al. (1996). Again, functions from Parton et al. (1996) are adapted for $Fr(NO_3)$, Fr(C), and Fr(θ), while Fr(pH) was modified from Dannenmann et al. (2008) and Rochester (2003).

$$Fr(NO_3) = 1 - \left[0.5 + \frac{1 * \text{atan}(\pi * 0.01 * (NO_3 - 190)}{\pi}\right] * 25 \quad (8)$$

$$Fr(C) = 13 + \frac{30.78 * a \tan(\pi * 0.07 * (C - 13))}{\pi} \quad (9)$$

Table 1
Soil texture fitting parameters for denitrification rate model (Parton et al., 1996).

Texture	a	b	c	d
Sand	1.56	12	16	2.01
Loam	4.82	14	16	1.39
Clay	60	18	22	1.06

$$Fr(\theta) = \frac{1.4}{13^{13^{\frac{17}{(2.2*\theta)}}}} \quad (10)$$

$$Fr(pH) = \frac{1}{1470*e^{-1.1*pH}} \quad (11)$$

Total N_2O production during denitrification is given by:

$$DN_2O = \frac{Dt}{1 + R_{N2/N20}} \quad (12)$$

where DN_2O is total N_2O flux per unit area in g N ha^{-1} d^{-1}.

N_2O emissions from nitrification were obtained by modifying the existing nitrification routine in SWAT and developing a set of equations for partitioning N_2O from NO_3^-. To calculate the total N_2O flux from nitrification an equation from (Parton et al., 1998, 2001) is used:

$$F_{N_2O} = F_{NO_3}*K_2*F_\theta*F_{Tmp}*F_{pH} \quad (13)$$

where F_{N_2O} is N_2O flux from nitrification (g N ha^{-1} d^{-1}), K_2 is the fraction of nitrified N lost as N_2O ($K_2 = 0.02$). F_{NO_3} is the rate of nitrification, F_θ is the effect of soil water on nitrification, F_{Tmp} is the effect of temperature, and F_{pH} is the effect of soil pH. Both F_{NO_3} and F_θ are taken directly from SWAT.

The F_{NO_3} factor is given by:

$$F_{NO_3} = \frac{f_{nit}}{f_{nit} + f_{vol}}*N_{nitvol} \quad (14)$$

where f_{nit} is the fraction of N lost to nitrification, f_{vol} is the fraction of N lost to volatilization and N_{nitvol} (g N ha^{-1} d^{-1}) is the amount of ammonium converted via nitrification and volatilization.

The $F_\theta$factor is given by:

$$F_\theta = \frac{SW_{ly} - WP_{ly}}{0.25*\left(FC_{ly} - WP_{ly}\right)} \text{ if } SW_{ly} < 0.25*FC_{ly} - 0.75*WP_{ly} \quad (15)$$

$$F_\theta = 1.0 \text{ if } SW_{ly} \geq 0.25*FC_{ly} - 0.75*WP_{ly} \quad (16)$$

where SW_{ly} is soil water content (mm), WP_{ly} is the amount of water held in the soil at wilting point water content (mm), and FC_{ly} is amount of water held in the soil layer at field capacity water content (mm).

The F_{Tmp}factor is given by:

$$F_{Tmp} = -0.06 + 0.13*e^{(0.07*SoilTemp)} \quad (17)$$

The F_{pH} factor is given by:

$$F_{pH} = 0.56 + \frac{\arctan(\pi*0.45*(-5 + soil\ pH))}{\pi} \quad (18)$$

The total N_2O production from both denitrification and nitrification is given by:

$$N_2O_{Total} = D_{N_2O} + F_{N_2O} \quad (19)$$

where N_2O_{Total} is total N_2O flux in g ha^{-1} d^{-1}.

2.3. Linking SWAT-GHG with SWAT parameters

All of the variables described above are already defined in SWAT and used in various other subroutines except for θ. θ is calculated from the soil moisture characteristics for each soil layer as the fraction of pore space occupied by water. Soil pH is included but is inactive in SWAT code and is a user-defined input. Thus for model development we used a constant soil pH over the user defined run time (note, however, that pH can be varied by the user during different model runs). In order to incorporate the impact of total soil C on N_2O emissions, the new N_2O routine utilizes one of two existing C routines in SWAT. In the basins.bsn file in SWAT, users can select the original routine from SWAT (nminrl.f) or a modified C routine (C-Farm) developed by Kemanian and Stöckle (2010). Note, the application that follows utilized the C-Farm routine.

2.4. Study area

SWAT-GHG was tested using plot level data from agricultural watersheds in West Lafayette, Indiana (Fig. 1a), and University Park, Pennsylvania (Fig. 1b). The watersheds have an area of 0.4 km^2 (Fig. 1a) and 0.6 km^2 (Fig. 1b), respectively. The crop types in University Park consist of corn, soybean, pasture and alfalfa, and West Lafayette crops consist of corn, soybean, sorghum and switchgrass. The soil type of the West Lafayette watershed is a loam, and the University Park watershed soil is a sandy clay loam.

2.5. Model testing

SWAT-GHG was tested using data from the GRACEnet database (http://nrrc.ars.usda.gov/arsdataportal/-/Home) at two locations: (1) University Park, Pennsylvania, and (2) West Lafayette, Indiana. SWAT-VSA (SWAT-Variable Source Area, Easton et al., 2008) was used for model testing. SWAT-VSA was initialized for both locations based on field level input data from the GRACEnet database to force the model where available. SWAT-VSA provided the soil moisture and temperature time series for the new routine, and all other inputs were taken from the GRACEnet database if available (soil properties) or left as default if unavailable (pH). In order to better understand which parameters had the largest effect on N_2O emissions we conducted a sensitivity analysis on N application rate, total soil C, pH, θ, and soil temperature.

2.6. Model initialization

SWAT-VSA was initialized for University Park and West Lafayette sites using ArcSWAT 2012 and TopoSWAT (available from http://ww2.bse.vt.edu/eastonlab/). TopoSWAT automates the SWAT-VSA initialization process by assimilating soil data, creating the TI map, overlaying the soil and TI maps, and developing the required database for model initialization (Fuka et al., 2016). Soils data included in TopoSWAT is based on Food and Agriculture Organization (FAO) soils database (FAO, 2003). The FAO soils were used as the base map and parameters (total soil C and N, soil texture) were adjusted using data provided in the GRACEnet database for each site. The land use input for both watersheds was obtained by first digitizing plot level land use based on the crop rotation of plots in the GRACEnet database. Digitized plot level land use data was then cross-referenced with data from the National Land Cover Database (Homer et al., 2012). The use of the NLCD was required because GRACEnet did not have all of the SWAT required soil, management, or plant growth and development parameters needed to run the model. A digital elevation model (DEM) with 10 m resolution from the United States Geologic Survey (USGS) National Elevation Dataset (NED) (Guenther & Maune, 2007) was used for both locations. The final initialization resulted in one subbasin with 58 HRUs for West Lafayette and one subbasin with 21 HRUs for University Park. Weather data from the GRACEnet database, including daily precipitation and temperature (min and max) from 2004 to 2013, was used to force the model. Soil properties such as organic C

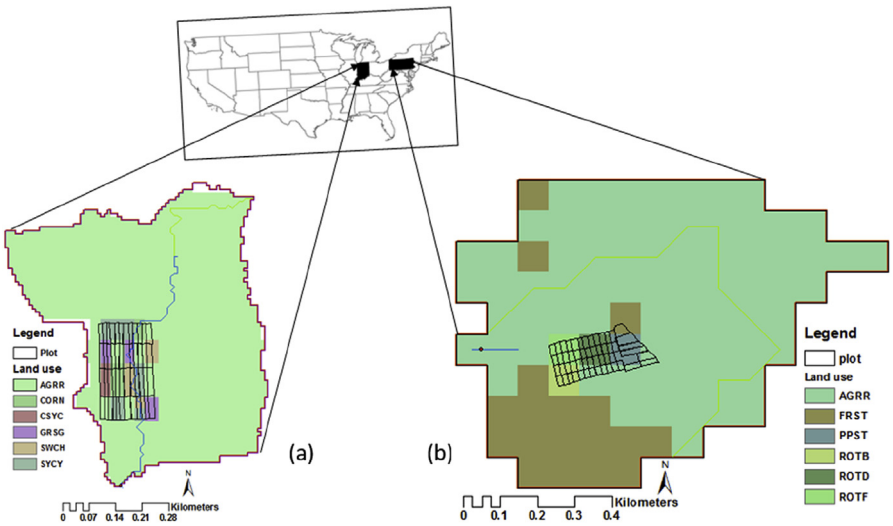

Fig. 1. (a) West Lafayette, IN, watershed and GRACEnet site with land uses AGRR (Agriculture); Corn; CSYC (Corn-Soybean-Corn crop rotation); GRSG (Sorghum); SWCH (Switchgrass); SYCY (Soybean-Corn-Soybean crop rotation) and (b) University Park, PA, watershed and GRACEnet site with land uses AGRR (Agriculture); FRST (Forest); PPST (Pasture); ROTB (Soybean rotation); ROTD (Alfalfa rotation); ROTF (Corn rotation).

content (%), soil NO_3^- content (mg kg^{-1}) and a default pH value of 6.5 from the FAO database were used to initialize both models.

2.7. GRACEnet database

GRACEnet (Greenhouse gas Reduction through Agricultural Carbon Enhancement network) is research program initiated by USDA Agricultural Research Service (ARS) to build high-quality data on trace gas fluxes in agroecosystems (Del Grosso et al., 2013). GRACEnet provides a site description, measured greenhouse gas fluxes, soil carbon levels, biomass yield, soil nutrient content, planting date, and fertilizer application rate, type and amount. Emission data are provided at a daily scale when measured, but measurements are periodic (e.g., measurements are made weekly). Thus we extract the model predicted fluxes on days that measurements are made for comparison. The spatial resolution is plot level, and measurements are made using the static chamber method where two chamber replicates are used per plot; detailed information about GRACEnet data can be found http://nrrc.ars.usda.gov/arsdataportal/#/Home.

2.8. Model calibration

There are many different methods to calibrate the SWAT model including genetic approaches, directional searches and evolutionary optimization (Zhang et al., 2016). However, given the complex crop rotations at the sites and the new variables introduced in SWAT-GHG both models were manually calibrated to the observed N_2O flux by changing the total soil C content in the first and second soil layers (as defined in the soils database), the amount and timing of N application in the management file, and the soil pH. Soil moisture and soil temperature were not used in the calibration since they were explicitly known and controlled by the measured precipitation and temperature.

2.9. Model corroboration

After manual calibration of both models, model performance was verified using subsequent time series data from 2011 to 2012 for West Lafayette and 2008 for University Park for respective crop types. Since the GRACEnet plots were managed under specific rotations, we corroborated both models by matching the crop rotation in the SWAT management files for those crop types that coincided between the calibration and corroboration time periods. Since there were multiple plots at each site managed under the same rotation (e.g., corn-soy) but at various stages in the rotation (e.g., one plot in the corn-soy rotation might be under corn in 2006 and another plot might be under soy), we extracted the modeled and observed N_2O fluxes that corresponded with each specific crop type by year and averaged the plot values together to create the time series of fluxes. As an example, in West Lafayette for the corn-soy rotation, the measured data started in 2008 and plot 1 was under soy, plot 2 was under corn and plot 3 was under soy, etc., so for 2008 soy fluxes consisted of measured and modeled data for plots 1 and 3 (averaged together), and corn for plot 2. In this manner, we iterated through each year sequentially extracting plot by crop fluxes to develop the time series of flux data. For each rotation year in the SWAT management file, where crop rotations are defined, we kept all calibrated parameters associated with each crop the same but changed the planting date and fertilizer application date according to the GRACEnet database and then reran the model.

There are many different model performance metrics available to test model skill (Bennett et al., 2013). Among different quantitative methods, the coefficient of determination (R^2) and Nash and Sutcliffe (1970) efficiency coefficient (NSE) are perhaps the most common (Moriasi et al., 2015), but both tend to evaluate the model skill in capturing the mean response. Since the extreme N_2O fluxes are of greater environmental importance, we include a performance metric that describes model performance at the extremes, namely the absolute maximum error (AME) (Bennett et al., 2013). The AME is a metric that indicates the maximum absolute deviation in the time series between measured and modeled data. Thus, the model skill was evaluated by comparing time series of simulated N_2O flux with observed N_2O flux data from the GRACEnet database and by comparing the predicted spatial distribution of emissions at the HRU level with the plot level N_2O emissions measured at each site.

2.10. Model sensitivity analysis (SA)

A model sensitivity analysis was performed on each model by

altering the initial conditions of the input parameters, including total soil C, N application rate, soil pH, air temperature (which subsequently alters soil temperature), and precipitation (which subsequently alters θ) by manually changing one variable at a time while keeping others unchanged (Norton, 2015; Pianosi et al., 2016; Saltelli & Annoni, 2010). Manual SA was chosen for several reasons 1) the relatively few number of HRUs and parameters of interest facilitated manual parameter adjustment and; 2) the most sensitive parameters can be easily identified. The SA was conducted by directly increasing or decreasing the C content by 10%, 20%, and 50% from the base model total soil C level, which resulted in a range of C contents typically found in agricultural soils for the two regions (0.6%–1.7% total soil C). In contrast, the soil N content was changed by increasing or decreasing the applied N (fertilizer application rate) in the management file by 10%, 20%, and 50% relative to the base model, which in turn altered the soil N level (3–10%). The soil pH was varied from the default value of 6.5 to pH 4, 5, 7, and 8. The sensitivity of the model to soil temperature and θ was assessed by increasing or decreasing the air temperature and precipitation, respectively, by 10%, 20%, and 30%, as the ± 50% adjustment was deemed outside the range of plausible conditions. A joint SA was calculated for applied N and pH as the model was shown to be most sensitive to their input.

3. Results

3.1. Sensitivity analysis

Model sensitivities were similar across all crop types; thus, we present SA results for the corn land use at both sites. Fig. 2 shows the results of the SA on N_2O and N_2 emissions for the University Park and West Lafayette sites. Both models were very sensitive to pH and applied N, moderately sensitive to soil temperature and precipitation, and relatively insensitive to total soil C content. At University Park, N_2O emissions increased by 65% and 46% as the pH was lowered from the base condition of 6.5 to 5 and 4, respectively, while emissions declined by 34% and 74% when the pH was raised from 6.5 to 7 and 8, respectively. At West Lafayette, N_2O emissions increased by 11% at pH 5, but decreased by 11%, 38%, and 70% at pH 4, 7, and 8, respectively. The model was also sensitive to the N application rate; higher N application rates resulted in higher N_2O emissions, up to 130% at University Park and 94% at West Lafayette when N application was increased by 50%, while decreases in N application rates reduced N_2O emissions by as much as 76% at University Park and 77% at West Lafayette when N application was decreased by 50% (Fig. 2). At the University Park site increasing temperature by 10% and 20% resulted in small increases in emissions (1–6%), while a 30% temperature increase reduced emissions by 1%. At West Lafayette decreasing temperature increased emissions (3–27%) while increasing temperature decreased emissions (15–18%). At University Park increases in precipitation decreased N_2O emissions slightly, 2–9%, while decreases in precipitation increased emissions 4–11% (Fig. 2). At West Lafayette both increase and decreases in precipitation tended to reduce emissions (1–15%). At both sites, increases in total soil C tended to increase N_2O emissions, while decreases in total soil C reduce N_2O emissions, although the magnitude of the changes was small (≤7%).

3.2. N_2O to N_2 comparison

Fig. 2a and b shows the breakdown of the modeled total daily denitrification products (N_2O and N_2) at University Park site and West Lafayette, respectively, for each level of the parameters tested in the SA. Since the model results were found to be particularly sensitive to pH and applied N, we present the results of a multi-level SA (Fig. 3a and b). In this analysis we varied applied N and pH together. Fig. 3a and b illustrates that increasing the soil pH while simultaneously increasing the soil N content dramatically increases the total denitrification rate and decreases the N_2O:N_2 product ratio. These figures demonstrate that, like N_2O emissions, both total denitrification and the ratio of denitrification products are most sensitive to pH followed by N application rate, and highlight the importance of both total flux and the product ratio in driving the differences in N_2O emissions presented in Fig. 2. For example, Fig. 2a and b shows that as pH increases total denitrification increases and the ratio N_2O:N_2 decreases. One exception to this is the lower level of denitrification observed at the University Park site at pH 7 compared to 8. While low pH is associated with higher N_2O emissions and higher N_2O:N_2 ratio (Fig. 3a and b), the lower emissions predicted at pH 4 relative to pH 5 at both sites are driven by the decrease in total denitrification, which overwhelms the ratio effect, and limits N_2O flux at pH 4. After pH, N application rate has the greatest effect not only on N_2O emissions, but also on total denitrification flux. The relationship between pH and total denitrification and N_2O production is the same at both sites, as is the effect of soil N content, as expected. Both sites demonstrate the expected correlation, where total denitrification, N_2O:N_2, and N_2O emissions increase as soil N content increases. Temperature increases tended to reduce N_2O emissions at both sites but there was no clear impact on N_2 or the product ratio due to changing temperature. Increasing or decreasing total soil C or precipitation had little effect on denitrification emissions or the product ratio at either site.

3.3. Model corroboration

Table 2 shows the NSE, R^2, and AME of the measured versus calibrated and corroborated model N_2O emissions for different crops at both test sites. The NSE values shows the model has good mean explanatory power for all crops at both test sites during the calibration period, with slightly lower, but still acceptable predictive power during the corroboration period. In terms of peak model prediction there is more variability; the model captures peak N_2O emissions generally well at both sites, but the AME indicated some peak error, some of which is due to mistimed peaks (e.g., corn at both sites) and some is due to under or over predicted peaks (e.g., soy at University Park, sorghum at West Lafayette, Figs. 4 and 6). Comparing each crop, the model predicted N_2O emissions best, as indicated by NSE value, for alfalfa followed by corn, soybean and pasture at University Park, and sorghum, followed by corn and soybean at West Lafayette. There was some reduced model performance during the corroboration periods at both sites, which is primarily due to averaging responses of different plots into one time series. Despite this, the models captured the timing and magnitude of N_2O emissions relatively well.

4. University Park, PA

4.1. Time series evaluation

The time series of measured and modeled N_2O emissions were compared for each crop type at the University Park site. The comparison between observed and simulated N_2O emissions for the corn crop (Fig. 4a) shows that the model captured both the magnitude and timing of emissions quite well in both the calibration and corroboration periods. For the soybean crop during the calibration period the model predicted the seasonal pattern of N_2O moderately well with a slight under estimation during July–September, although the peaks are well predicted (Fig. 4b). During the corroboration period the timing of emission peaks is well captured,

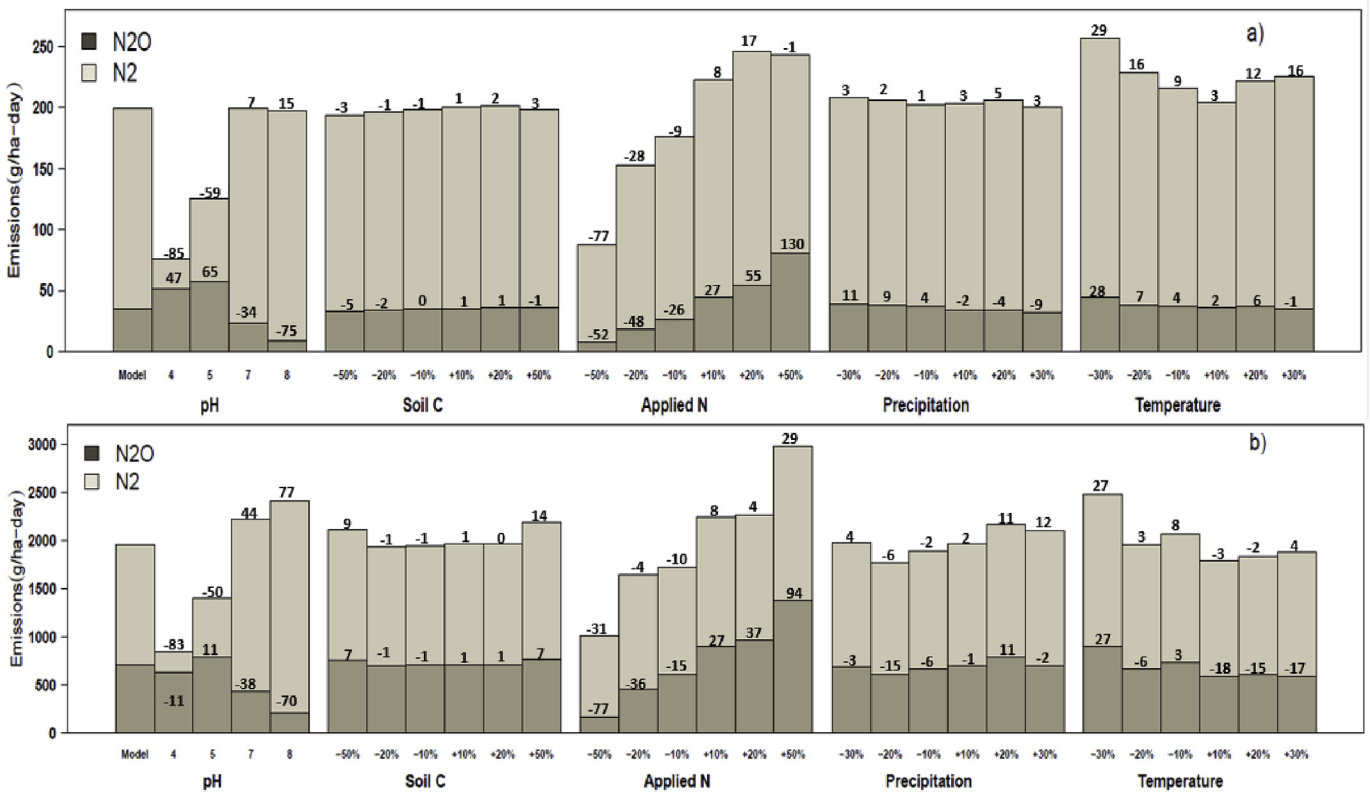

Fig. 2. Comparison of model output N_2O and N_2 (from both nitrification and denitrification) for different soil and environmental factors and percent change (over each bar) from the base model at the University Park site (a) and the West Lafayette site (b) for the corn land use. The base model parameter values for the University Park site are: pH = 6.5, total soil C % = 1.7 for the first soil layer and 0.7 for the second soil layer; mean temperature = 10 °C, mean yearly precipitation = 1035 mm, and soil N = 650 kg ha^{-1}. The initial model parameters for West Lafayette site are: pH = 6.5, total soil C % = 1.6 for the first soil layer and 0.7 for the second soil layer, mean daily temperature = 11.8 °C, mean yearly precipitation = 1174 mm, and soil N = 1800 kg ha^{-1}.

but the June event is over predicted (Fig. 4b). For alfalfa the model predicted both the timing and peak values well during the calibration period, particularly following the fertilizer applications in May, June, and August (Fig. 4c). During the corroboration period emission timing was well captured, but the event in April was over predicted (Fig. 4c). For pasture (Fig. 4d) in both the calibration and corroboration periods the model tended to under estimate the peaks but captured the timing and lower emissions well.

4.2. Spatial evaluation

Fig. 5 shows the measured and predicted spatial distribution of N_2O emissions for the University Park site. In general, the model was able to predict the distribution of emission well, both spatially and in magnitude. The model tended to slightly over predict emissions from pasture (by about 15%), but corn, alfalfa, and soybean emissions were well predicted across the site, with less than a 10% difference (Fig. 5).

5. West Lafayette, IN

5.1. Time series evaluation

The time series evaluation between observed and simulated N_2O emissions for different crop types examines 2008 to 2010 for the calibration period and 2011 for the corroboration period. For corn, the model captured the magnitude of the peaks quite well during the calibration period, despite missing the timing of the peaks slightly in June 2008 and 2010 (Fig. 6a). During the corroboration period the event timing was well predicted but the magnitude was slightly under predicted (Fig. 6a). Emissions from the soybean crop (Fig. 6b) were well predicted during the calibration and corroboration periods. Fig. 6c shows model predicted N_2O emissions for sorghum and that it was able capture the seasonal pattern of emissions, despite some underestimated peaks in both the calibration and corroboration periods.

5.2. Spatial evaluation

Fig. 7 shows the measured and predicted spatial distribution of N_2O emissions for the West Lafayette site. Similar to the University Park site the model generally predicted both the spatial distribution and magnitudes of emission well across the fields (Fig. 7). The corn and corn-soybean rotation were slightly more accurately predicted than the sorghum crop. The West Lafayette site exhibited variability between crop types and between plots than at University Park, which the model is able to capture. For instance, corn had measured emissions ranging from <5 to 50 g ha^{-1} at West Lafayette (Fig. 7) while the range at University Park was 22–50 g ha^{-1} (Fig. 6). Clearly the model is able to capture the spatial distribution of N_2O hotspots quite well.

6. Discussion

6.1. Modeling the environmental controls on N_2O and N_2 emissions

pH: N_2O emissions were by far the most sensitive to changes in pH (Figs. 2 and 3), and it is reassuring that the model was able to

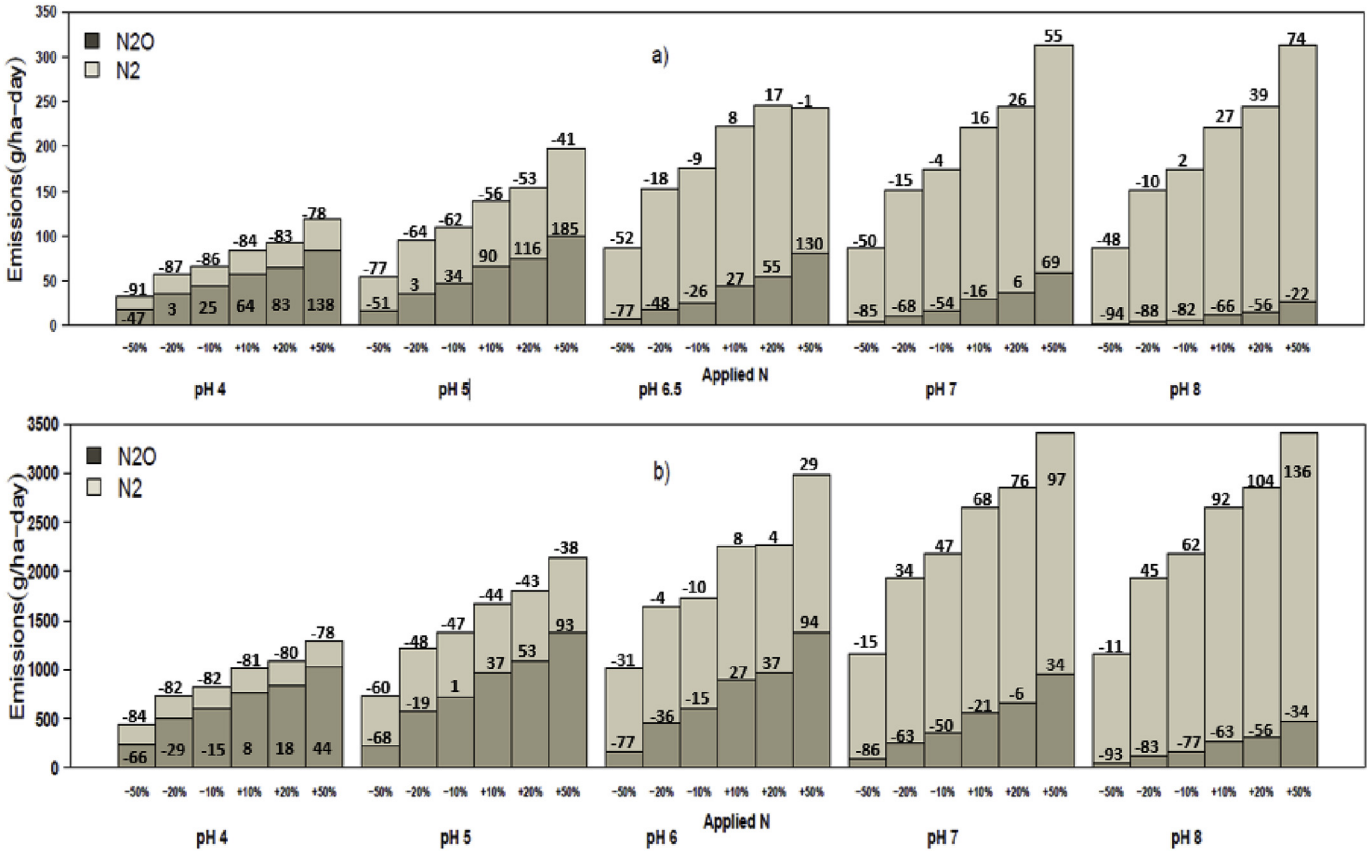

Fig. 3. Comparison of model output N_2O and N_2 (from both nitrification and denitrification) and percent change (over each bar) against the base model in Fig. 2 for simultaneous changes in applied N and pH at the University Park site (a) and the West Lafayette site (b) for the corn land use.

Table 2
R-squared values (R^2), Nash-Sutcliffe coefficients (NSE), and absolute maximum error (AME) and for the calibrated model for all crop types at both test sites, University Park and West Lafayette. Note that the variables that were calibrated were the soil pH, N application rate, and total soil C level, and all others remained as defaults from the GRACEnet database or SWAT initialization.

Site	Crop	Calibration			Corroboration		
		R^2	NSE	AME	R^2	NSE	AME
University Park	Corn	0.67	0.65	95.0	0.51	0.44	45.2
	Alfalfa	0.95	0.86	9.0	0.48	0.42	26.0
	Soybean	0.81	0.56	39.2	0.42	0.24	95.7
	Pasture	0.52	0.51	51.6	0.60	0.51	39.3
West Lafayette	Corn	0.74	0.73	2953.7	0.70	0.41	2765.6
	Soybean	0.69	0.48	299.5	0.73	0.34	116.5
	Sorghum	0.80	0.78	426.8	0.48	0.44	309.7

capture this effect because pH has long been known to exert both proximal and distal control on emissions (Mørkved et al., 2007). Some of this effect is due to the proximal control (enzyme and substrate level effects) of pH on N_2O reducing enzymes, which are more sensitive to low pH than the enzymes that reduce NO_3^- and NO_2^-; the former being more active at pH > 7 and the latter more active at pH < 7 (Richardson et al., 2009). Thus, N_2O is produced at low pH but is not converted to N_2 and tends to build up in the system because the activity of nitrous oxide reductase is inhibited. In most soils N_2O emissions are smallest at neutral to basic pH (Liu et al., 2010), and our model predicts this; at a pH of 8 emissions were between 70% and 74% lower than at pH 6.5, although total denitrification was greater (Figs. 2 and 3), and decreasing pH generally increased the N_2O:N_2 ratio (Figs. 2 and 3). These results reflect the importance of pH not only as a dominant control on total denitrification, but also on the composition of the products; at pH values between 4 and 8, the ratio N_2O:N_2 increases as pH decreases, and below pH 4 denitrification is largely inhibited due to negative impacts on denitrifying enzyme synthesis (Liu et al., 2010). Interestingly, at both sites the highest emissions N_2O were predicted to occur at a pH of 5 (University Park, 58 g ha^{-1} d^{-1} and West Lafayette, 787 g ha^{-1} d^{-1}) rather than at pH 4 (University Park, 51 g ha^{-1} d^{-1} and West Lafayette, 630 g ha^{-1} d^{-1}), as might be expected. This is because total denitrification ($N_2 + N_2O$) was higher at pH 5 than pH 4, so despite the higher N_2O:N_2 at pH 4, the quantity of N_2O emitted at pH 4 was less than at pH 5 (Figs. 2 and 3). While total denitrification and N_2O:N_2 were significantly higher at the West Lafayette site for the corn land use in the base model and all conditions tested in the SA compared to University Park, the effect of pH on denitrification gas flux is consistent between research sites and with the literature (e.g., Mørkved et al., 2007; Liu et al., 2010; Richardson et al., 2009).

Soil C:N Ratio: Altering total soil C levels by ± 10%, 20%, and 50% had little impact on N_2O emissions, which is somewhat surprising given that both systems were C-limited under all of the scenarios tested (e.g., initial C:N ratios 2.6:1 for PA and 1:0.8 for IN). Generally C:N ratios <20:1 are considered C-limited (Richardson et al., 2009), so an increase in the C content would be expected to increase the denitrification rate. However, changing C levels resulted in very little change in emissions at either site (−5%–3% in PA, and 5%–7% in IN). With such low soil C:N ratios at the study sites, N_2O emissions may have been overwhelmed by the effect of the relatively high N content of the soil; high NO_3^- concentrations can inhibit N_2O reduction as NO_3^- serves as an electron acceptor energetically

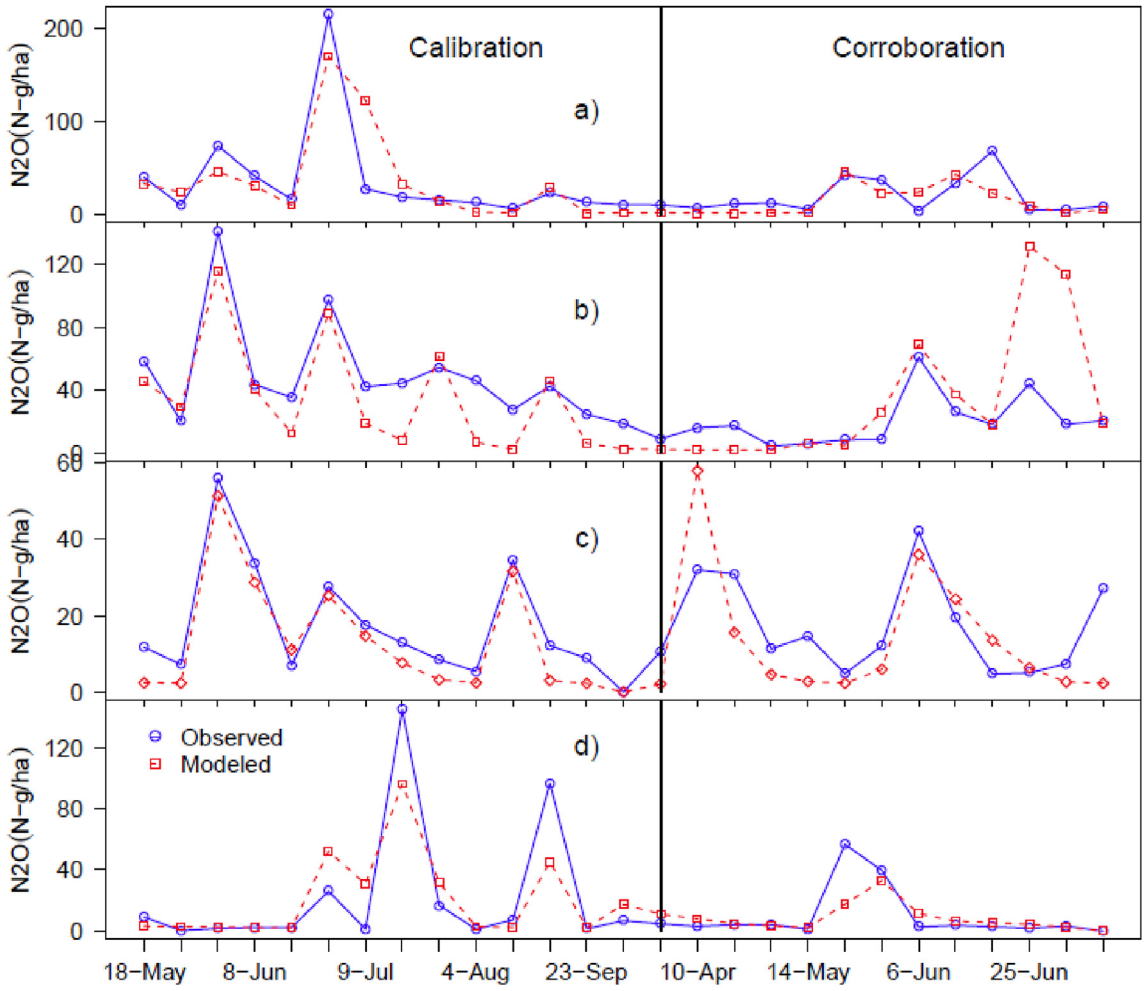

Fig. 4. Comparison of observed and modeled N_2O emissions for the University Park site for 2006 during calibration and 2008 for corroboration; (a) Corn, (b) Soybean, (c) Alfalfa, and (d) Pasture.

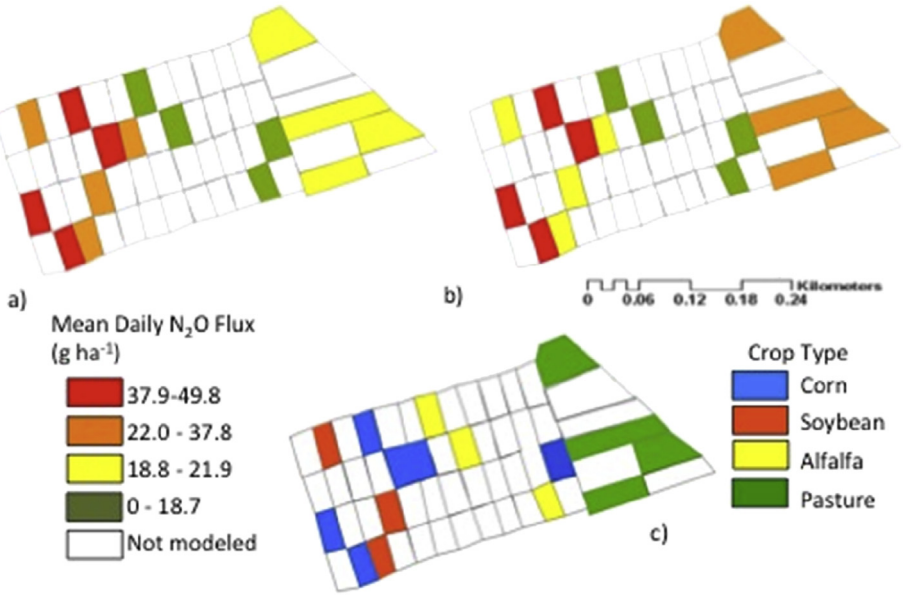

Fig. 5. Spatial comparison of daily average N_2O emissions for the University Park site for 2008, (a) measured N_2O flux, (b) modeled N_2O flux, (c) crop types where measurements were made. The overlay polygon map shows the field layout for the site. Unpredicted plots are those for which GRACEnet N_2O measurements were unavailable, where we could not match the rotations or the crop type did not exist in the SWAT crop database.

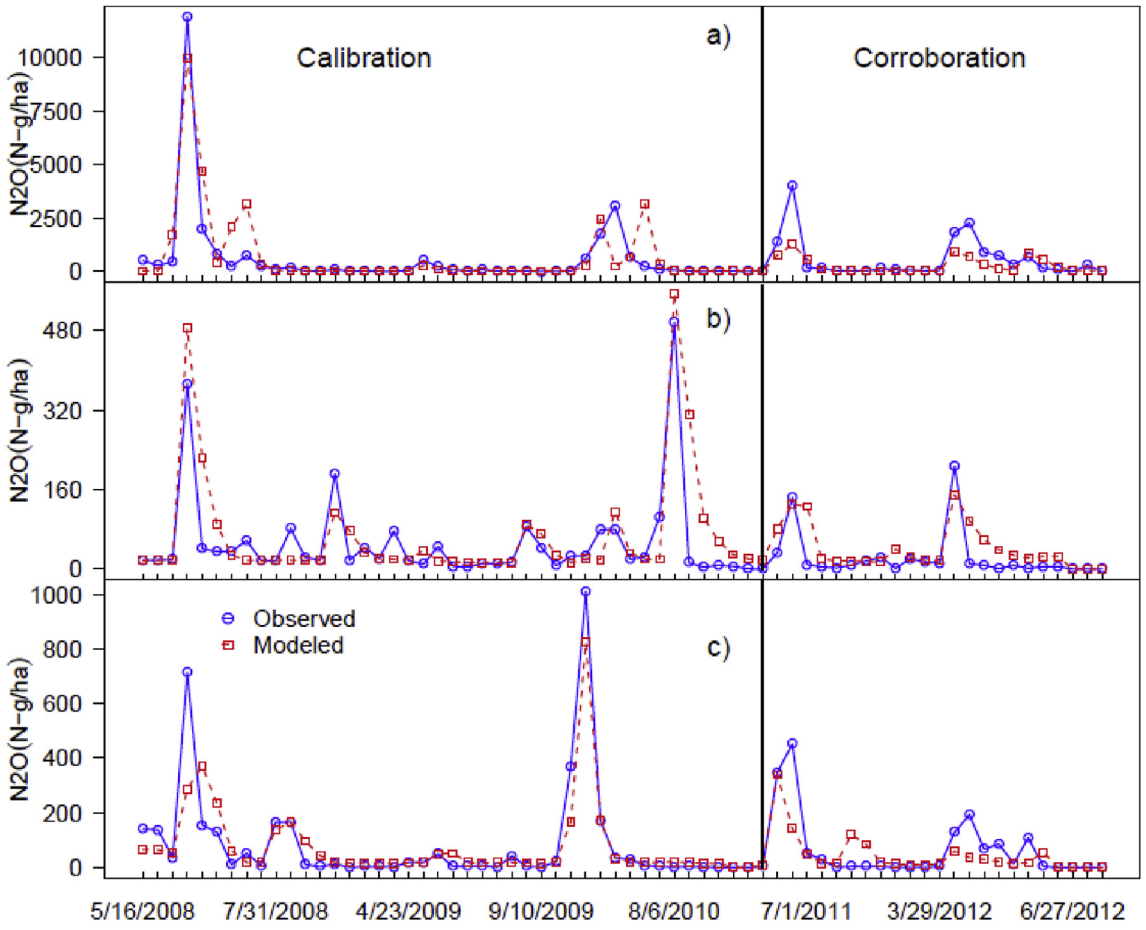

Fig. 6. Comparison of observed and modeled N_2O emissions for West Lafayette, 2008 to 2010 for calibration and 2011 to 2012 for corroboration for (a) Corn, (b) Soybean, and c) Sorghum.

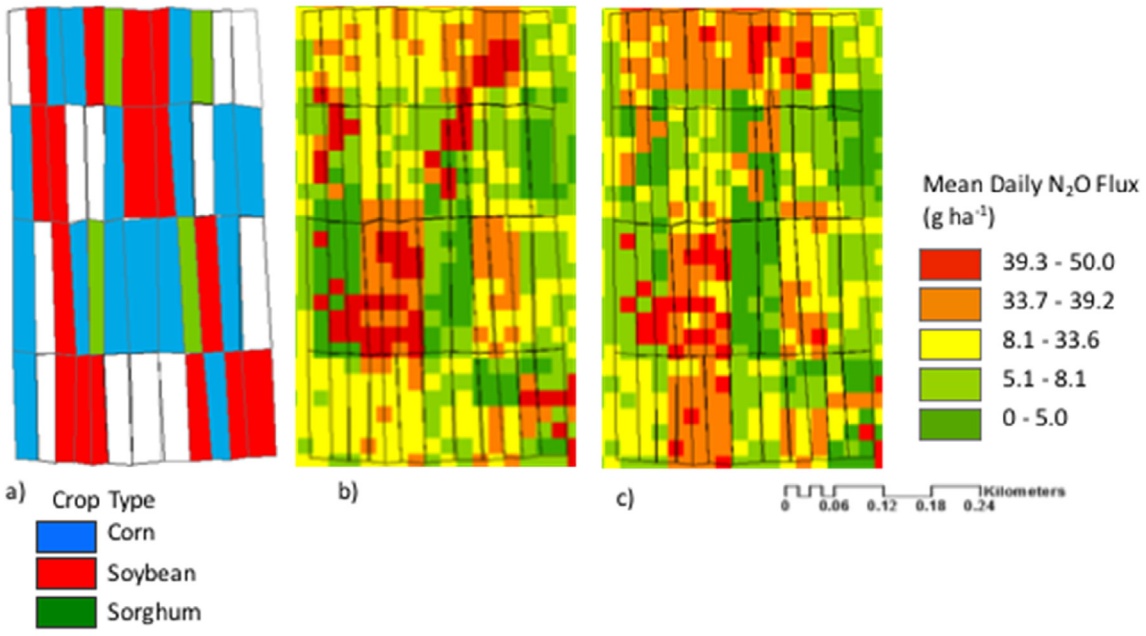

Fig. 7. Spatial comparison of daily average N_2O emissions for West Lafayette test site for 2011, (a) measured N_2O flux, (b) modeled N_2O flux, (c) crop types where measurements were made. Unpredicted plots are those for which GRACEnet N_2O measurements were unavailable, rotations could not be matched or the crop type did not exist in SWAT. Note that multiple HRUs can occur in a single field due to differences in soil type and topography.

preferable to N_2O. Indeed, emission were much more sensitive to the N application rate imparting a −76%–130% change on emissions at University Park and −77%–94% change at West Lafayette (Fig. 2). With respect to denitrification, the importance of the N application rate and by extension the soil N content is well established (Hai et al., 2009; Saggar et al., 2013) and the clear correlation between the N application rate and both total denitrification and N_2O emissions was as expected under C-limited conditions.

Temperature: Generally, increases in microbial activity are predicted as temperatures increase, but complex interactions among microbial processes that may be competing for soil nutrients make the net results difficult to predict. For example, some research has shown that increasing temperatures promote complete denitrification (reduction to N_2 rather than halting at N_2O), which could reduce N_2O emissions (Stres et al., 2008), but increasing temperatures also increase overall microbial activity, which could increase emissions of both products. Indeed, the results of our simulations with respect to increased temperature (Fig. 2) suggest complex interactions, where moderate increases in temperature (+10% and 20%) at University Park slightly increased emissions (1–6%) but the 30% temperature increase actually decreased emissions 1%. At West Lafayette increases in temperatures decreased emissions (15–18%). Decreases in temperature at both sites increased N_2O emissions 3–28% (Fig. 2). N_2 and total denitrification (Fig. 2) are similarly affected, the highest total denitrification and N_2 emissions occur at a 30% decrease in temperature. The responses to temperature at the two sites may be reflective of differences in the soil types (sandy clay loam at University Park and loam at West Lafayette) and soil moisture status (precipitation quantity and timing differing between the sites) that affect how changes in air temperature translate to changes in the soil temperature (e.g., there is a dampened lag).

Soil Moisture, θ: Changes in θ do not produce a linear nor directionally consistent response in N_2O emissions. Changes in θ can cause rapid shifts between nitrification and denitrification (Bergsma et al., 2002; Webster & Hopkins, 1996). As θ decreases pore space oxygen concentrations increase, most denitrification to ceases, and nitrification rapidly becomes the dominant N transformation process. Return to anaerobic conditions causes a similar reversal to denitrification. These periods of transition often coincide with peak periods of N_2O flux, especially in agricultural soils (Butterbach-Bahl & Dannenmann, 2011). Indeed, the effect of soil moisture on N_2O emissions in Fig. 2 could be partially explained by the temporal dynamics of soil wetting/drying. However, while more frequent wetting and drying at University Park (data not shown) might lead us to expect higher N_2O emissions, the N_2O:N_2 ratio is higher at West Lafayette, presumably due to the greater soil N levels at West Lafayette (1800 kg ha^{-1} compared to 650 kg ha^{-1} at University Park), the higher levels of total denitrification, about ten times greater than University Park, are expected.

All of these factors interact in complex ways, which limits the value of conclusions drawn from assessing their individual impact. For instance, temperature affects C:N ratio by changing the rate of C decomposition and N cycling. Temperature also alters θ by changing evapotranspiration and plant moisture uptake. Increasing total soil C can also increase the water holding capacity of the soil and in turn increase θ as well. An integrated model capable of capturing these complex interactions is one of the only ways to assess how N_2O emissions change under altered environmental conditions. SWAT-GHG was able to reliably predict how these factors affect N_2O emission and is thus useful for assessing the impact of targeted landscape management on N_2O emissions.

Implications for Modeling: Accurate prediction of the spatial and temporal extent of GHG emissions is critical for managing agricultural nutrients. Despite some discrepancies in the timing or magnitude of peak N_2O emissions (e.g., Figs. 4 and 6), SWAT-GHG simulated N_2O emissions well at both sites. The reason for discrepancies might be due to the several factors; 1) the dynamic nature of N_2O emissions that can vary dramatically over the course of a day [e.g., the model integrates over a 24 h period, while the measurements integrate over a 1 h period (Parkin & Venterea, 2010)]; 2) the uncertainty in the input data (e.g., amount and time of application of fertilizer, soil pH, missed precipitation event); or 3) process conceptualization in the model itself. However, compared to other denitrification/N_2O models SWAT-GHG simulated the spatial and temporal N_2O emissions from agroecosystems as well or better than most other models in the literature. For instance, Parton et al. (2001) who developed DAYCENT were able to simulate annual and monthly N_2O emissions well but daily emissions were poorly predicted; the authors speculate that this is due to the effect of topography redistributing soil moisture, which DAYCENT was not developed to capture. Morse et al. (2012) suggest that finer temporal (and spatial) scale models that can capture the variability of N_2O emission are critical to better managing landscape scale GHG emissions. SWAT-GHG provides these enhanced simulation capabilities for agroecosystems by linking the effect of topography (SWAT-GHG is based on the SWAT-VSA model which incorporates the impact of topography) and the processes controlling GHG emissions. Indeed, the incorporation of more mechanistic soil moisture predictions represents an improvement on previous modeling efforts. Although the model generally simulates N_2O emissions well, there are some areas where the model could be improved, such as including dynamic soil pH calculation (e.g., currently pH in is a user defined, static input). Addition of dynamic pH would allow the quantification of the impact of management practices, such as liming and/or use of acidifying fertilizers, on N_2O emissions over time.

SWAT-GHG can be used and applied to agroecosystems at a range of scales, crop types and management regimes and used to test scenarios related to crop production, agricultural best management practices and climate change. This would allow managers to identify areas of the landscape that have a high emissions and a high potential for management practices to reduce emissions. For instance, the model can be used to assess the impacts of management practices such as tillage, drainage water management, nutrient management, and soil amendments on GHG emissions or for assessing the impact of climate change on N_2O emissions.

7. Conclusions

This paper describes SWAT-GHG, a new routine for the SWAT model to predict N_2O emissions in agroecosystems using soil and environmental factors such as soil N and C content, soil temperature, soil pH, and soil θ as the controlling factors. The base model upon which SWAT-GHG was developed incorporates the impact of topography on the redistribution on soil water. The model was tested for different crop types and compared with measured N_2O values at two test sites: University Park, PA and West Lafayette, IN. The model simulated N_2O well in both time and space as verified by comparison to measured N_2O flux from different crop types. Perhaps more importantly, the model was sensitive to changes in soil and environmental factors such as soil pH, soil nutrient content and precipitation. This new model represents an advance over many existing GHG emission models in several respects; 1) it incorporates the physical processes controlling N_2O emissions; 2) it uses easily available input parameters to initialize; 3) it provides predictions at the subfield scale; and 4) it is able to capture emission at a high temporal frequency.

Acknowledgements

This research is based on work supported by the National Science Foundation (NSF) under Grant No. CBET-1360280.

References

Arah, J.R.M., Smith, K.A., 1989. Steady state denitrification in aggregated soils-a mathematical model. J. Soil Sci. 40 (1), 139–149.

Arnold, J.G., Srinivasan, R., Muttiah, R.S., Williams, J.R., 1998. Large area hydrologic modeling and assessment part I: model development. J. Am. Water Resour. Assoc. 34 (1), 73–89. http://dx.doi.org/10.1111/j.1752-1688.1998.tb05961.x.

Beheydt, D., Boeckx, P., Ahmed, H.P., Van Cleemput, O., 2008. N2O emission from conventional and minimum-tilled soils. Biol. Fertil. Soils 44 (6), 863–873. http://dx.doi.org/10.1007/s00374-008-0271-9.

Bennett, N.D., Croke, B.F.W., Guariso, G., Guillaume, J.H.A., Hamilton, S.H., Jakeman, A.J., Marsili-Libelli, S., Newham, L.T.H., Norton, J.P., Perrin, C., Pierce, S.A., Robson, B., Seppelt, R., Voinov, A.A., Fath, B.D., Andreassian, V., 2013. Characterising performance of environmental models. Environ. Model. Softw. 40, 1–20. http://dx.doi.org/10.1016/j.envsoft.2012.09.011.

Bergsma, T.T., Robertson, G.P., Ostrom, N.E., 2002. Influence of soil moisture and land use history on denitrification end-products. J. Environ. Qual. 31 (3), 711–717.

Bruland, G.L., Richardson, C.J., Whalen, S.C., 2006. Spatial variability of denitrification potential and related soil properties in created, restored, and paired natural wetlands. Wetlands 26 (4), 1042–1056. http://dx.doi.org/10.1672/0277-5212(2006)26[1042:svodpa]2.0.co;2.

Butterbach-Bahl, K., Dannenmann, M., 2011. Denitrification and associated soil N2O emissions due to agricultural activities in a changing climate. Curr. Opin. Environ. Sustain. 3 (5), 389–395. http://dx.doi.org/10.1016/j.cosust.2011.08.004.

Clement, J.C., Pinay, G., Marmonier, P., 2002. Seasonal dynamics of denitrification along topohydrosequences in three different riparian wetlands. J. Environ. Qual. 31 (3), 1025–1037. http://dx.doi.org/10.2134/jeq2002.1025.

Dannenmann, M., Butterbach-Bahl, K., Gasche, R., Willibald, G., Papen, H., 2008. Dinitrogen emissions and the N2:N2O emission ratio of a Rendzic Leptosol as influenced by pH and forest thinning. Soil Biol. Biochem. 40 (9), 2317–2323. http://dx.doi.org/10.1016/j.soilbio.2008.05.009.

Del Grosso, S., Ojima, D., Parton, W., Mosier, A., Peterson, G., Schimel, D., 2002. Simulated effects of dryland cropping intensification on soil organic matter and greenhouse gas exchanges using the DAYCENT ecosystem model. Environ. Pollut. 116, S75–S83. http://dx.doi.org/10.1016/s0269-7491(01)00260-3.

Del Grosso, S., White, J., Wilson, G., Vandenberg, B., Karlen, D., Follett, R., Johnson, J., Franzluebbers, A., Archer, D., Gollany, H., 2013. Introducing the GRACEnet/REAP data contribution, discovery, and retrieval system. J. Environ. Qual. 42 (4), 1274–1280.

Easton, Z.M., Fuka, D.R., Walter, M.T., Cowan, D.M., Schneiderman, E.M., Steenhuis, T.S., 2008. Re-conceptualizing the soil and water assessment tool (SWAT) model to predict runoff from variable source areas. J. Hydrol. 348 (3), 279–291. http://dx.doi.org/10.1016/j.jhydrol.2007.10.008.

Fang, Q., Ma, L., Halvorson, A., Malone, R., Ahuja, L., Del Grosso, S., Hatfield, J., 2015. Evaluating four nitrous oxide emission algorithms in response to N rate on an irrigated corn field. Environ. Model. Softw. 72, 56–70.

FAO-AGL, 2003. WRB Map of World Soil Resources. Land and Water Development Division, Food and Agriculture Organization of the United Nations. Available at: http://www.fao.org/ag/agl/agll/wrb/soilres.stm. last access: June 2010.

Frolking, T.A., Changsheng, L.I., Frolking, S., 1992. A model of nitrous oxide evolution from soil driven by rainfall events. I - model structure and sensitivity. II - model applications. J. Geophys. Res. 97 (D9).

Fuka, D.R., Auerbach, D., Collick, A.S., Easton, Z.M., 2016. The TopoSWAT toolbox: Enhanced basin characterization in SWAT initializations. Environ. Model. Softw. (In Review).

Grant, R.F., 1991. A technique for estimating denitrification rates at different soil temperatures, water contents, and nitrate concentrations. Soil Sci. 152 (1), 41–52. http://dx.doi.org/10.1097/00010694-199107000-00007.

Groffman, P.M., Butterbach-Bahl, K., Fulweiler, R.W., Gold, A.J., Morse, J.L., Stander, E.K., Tague, C., Tonitto, C., Vidon, P., 2009. Challenges to incorporating spatially and temporally explicit phenomena (hotspots and hot moments) in denitrification models. Biogeochemistry 93 (1/2), 49–77. http://dx.doi.org/10.1007/s10533-008-9277-5.

Guenther, G., Maune, D., 2007. Digital Elevation Model Technologies and Applications: the DEM Users Manual. Airborne LiDAR bathymetry, second ed. American Society for Photogrammetry and Remote Sensing, USA, pp. 253–320.

Hai, B., Diallo, N.H., Sall, S., Haesler, F., Schauss, K., Bonzi, M., Assigbetse, K., Chotte, J.-L., Munch, J.C., Schloter, M., 2009. Quantification of key genes steering the microbial nitrogen cycle in the rhizosphere of sorghum cultivars in tropical agroecosystems. Appl. Environ. Microbiol. 75 (15), 4993–5000.

Hansen, S., Jensen, H.E., Nielsen, N.E., Svendsen, H., 1991. Simulation of nitrogen dynamics and biomass production in winter-wheat using the Danish simulation model DAISY. Fertil. Res. 27 (2–3), 245–259. http://dx.doi.org/10.1007/BF01051131.

Heinen, M., 2006. Simplified denitrification models: overview and properties. Geoderma 133 (3), 444–463. http://dx.doi.org/10.1016/j.geoderma.2005.06.010.

Henault, C., Germon, J.C., 2000. NEMIS, a predictive model of denitrification on the field scale. Eur. J. Soil Sci. 51 (2), 257–270. http://dx.doi.org/10.1046/j.1365-2389.2000.00314.x.

Homer, C.H., Fry, J.A., Barnes, C.A., 2012. The national land cover database. US Geol. Survey Fact Sheet 3020 (4), 1–4.

Jahangir, M.M.R., Johnston, P., Addy, K., Khalil, M.I., Groffman, P.M., Richards, K.G., 2013. Quantification of in situ denitrification rates in groundwater below an arable and a grassland system. Water, Air, & Soil Pollut. 224 (9), 1–14. http://dx.doi.org/10.1007/s11270-013-1693-z.

Kelly, R.A., Jakeman, A.J., Barreteau, O., Borsuk, M.E., ElSawah, S., Hamilton, S.H., Henriksen, H.J., Kuikka, S., Maier, H.R., Rizzoli, A.E., van Delden, H., Voinov, A.A., 2013. Selecting among five common modelling approaches for integrated environmental assessment and management. Environ. Model. Softw. 47, 159–181. http://dx.doi.org/10.1016/j.envsoft.2013.05.005.

Kemanian, A.R., Stöckle, C.O., 2010. C-Farm: a simple model to evaluate the carbon balance of soil profiles. Eur. J. Agron. 32 (1), 22–29. http://dx.doi.org/10.1016/j.eja.2009.08.003.

Knowles, R., 1982. Denitrification. Microbiol. Rev. 46 (1), 43–70.

Kragt, M.E., Newham, L.T.H., Bennett, J., Jakeman, A.J., 2011. An integrated approach to linking economic valuation and catchment modelling. Environ. Model. Softw. 26 (1), 92–102. http://dx.doi.org/10.1016/j.envsoft.2010.04.002.

Leffelaar, P.A., 1988. Dynamics of partial anaerobiosis, denitrification, and water in a soil aggregate. Soil Sci. 146 (6), 427–444. http://dx.doi.org/10.1097/00010694-198812000-00004.

Leffelaar, P.A., Wessel, W.W., 1988. Denitrification in a homogeneous, closed system. Soil Sci. 146 (5), 335–349. http://dx.doi.org/10.1097/00010694-198811000-00006.

Li, C., Frolking, S., Crocker, G.J., Grace, P.R., Klír, J., Körchens, M., Poulton, P.R., 1997. Simulating trends in soil organic carbon in long-term experiments using the DNDC model. Geoderma 81 (1), 45–60. http://dx.doi.org/10.1016/S0016-7061(97)00080-3.

Li, Y., White, R., Chen, D., Zhang, J., Li, B., Zhang, Y., Huang, Y., Edis, R., 2007. A spatially referenced water and nitrogen management model (WNMM) for (irrigated) intensive cropping systems in the North China Plain. Ecol. Model. 203 (3), 395–423. http://dx.doi.org/10.1016/j.ecolmodel.2006.12.011.

Liu, B., Mørkved, P.T., Frostegård, Å., Bakken, L.R., 2010. Denitrification gene pools, transcription and kinetics of NO, N2O and N2 production as affected by soil pH. FEMS Microbiol. Ecol. 72 (3), 407–417.

Metivier, K.A., Pattey, E., Grant, R.F., 2009. Using the ecosys mathematical model to simulate temporal variability of nitrous oxide emissions from a fertilized agricultural soil. Soil Biol. Biochem. 41 (12), 2370–2386. http://dx.doi.org/10.1016/j.soilbio.2009.03.007.

Moriasi, D.N., Gitau, M.W., Pai, N., Daggupati, P., 2015. Hydrologic and water quality models: performance measures and evaluation criteria. Trans. ASABE 58 (6), 1763–1785.

Mørkved, P.T., Dörsch, P., Bakken, L.R., 2007. The N_2O product ratio of nitrification and its dependence on long-term changes in soil pH. Soil Biol. Biochem. 39 (8), 2048–2057.

Morse, J.L., Ardón, M., Bernhardt, E.S., 2012. Using environmental variables and soil processes to forecast denitrification potential and nitrous oxide fluxes in coastal plain wetlands across different land uses. J. Geophys. Res. Biogeosci. 117 (G2) http://dx.doi.org/10.1029/2011JG001923 n/a-n/a.

Mosier, A.R., Doran, J.W., Freney, J.R., 2002. Managing soil denitrification. J. Soil Water Conserv. 57 (6), 505–513.

Nash, J.E., Sutcliffe, J.V., 1970. River flow forecasting through conceptual models. Part I a discussion of principles. J. Hydrol. 10, 282–290.

Norton, J., 2015. An introduction to sensitivity assessment of simulation models. Environ. Model. Softw. 69, 166–174. http://dx.doi.org/10.1016/j.envsoft.2015.03.020.

Parkin, T.B., Venterea, R.T., 2010. Sampling protocols. Chapter 3. Chamber-based trace gas flux measurements. In: Follett, R.F. (Ed.), Sampling Protocols, pp. 3–1 to 3-39. Available at: www.ars.usda.gov/research/GRACEnet.

Parton, W.J., Hartman, M., Ojima, D., Schimel, D., 1998. DAYCENT and its land surface submodel: description and testing. Glob. Planet. Change 19 (1), 35–48. http://dx.doi.org/10.1016/S0921-8181(98)00040-X.

Parton, W.J., Holland, E.A., Del Grosso, S.J., Hartman, M.D., Martin, R.E., Mosier, A.R., Ojima, D.S., Schimel, D.S., 2001. Generalized model for NOxand N2O emissions from soils. J. Geophys. Res. Atmos. 106 (D15), 17403–17419. http://dx.doi.org/10.1029/2001jd900101.

Parton, W.J., Mosier, A.R., Ojima, D.S., Valentine, D.W., Schimel, D.S., Weier, K., Kulmala, A.E., 1996. Generalized model for N2and N2O production from nitrification and denitrification. Glob. Biogeochem. Cycles 10 (3), 401–412. http://dx.doi.org/10.1029/96gb01455.

Pianosi, F., Beven, K., Freer, J., Hall, J.W., Rougier, J., Stephenson, D.B., Wagener, T., 2016. Sensitivity analysis of environmental models: a systematic review with practical workflow. Environ. Model. Softw. 79, 214–232. http://dx.doi.org/10.1016/j.envsoft.2016.02.008.

Priesack, E., Achatz, S., Stenger, R., 2001. Parameterization of Soil Nitrogen Transport Models by Use of Laboratory and Field Data. Modeling Carbon and Nitrogen Dynamics for Soil Management. CRC Press Inc., Boca Raton, Florida, pp. 461–484.

Richardson, D., Felgate, H., Watmough, N., Thomson, A., Baggs, E., 2009. Mitigating release of the potent greenhouse gas N_2O from the nitrogen cycle–could enzymic regulation hold the key? Trends Biotechnol. 27 (7), 388–397.

Riley, W., Matson, P., 2000. NLOSS: a mechanistic model of denitrified N2O and N2 evolution from soil. Soil Sci. 165 (3), 237–249.

Rochester, I.J., 2003. Estimating nitrous oxide emissions from flood-irrigated alkaline grey clays. Aust. J. Soil Res. 41 (2), 197–206. http://dx.doi.org/10.1071/SR02068.

Saggar, S., Jha, N., Deslippe, J., Bolan, N.S., Luo, J., Giltrap, D.L., Kim, D.G., Zaman, M., Tillman, R.W., 2013. Denitrification and N2O: N2 production in temperate grasslands: processes, measurements, modelling and mitigating negative impacts. Sci. Total Environ. 465, 173–195. http://dx.doi.org/10.1016/j.scitotenv.2012.11.050.

Saltelli, A., Annoni, P., 2010. How to avoid a perfunctory sensitivity analysis. Environ. Model. Softw. 25 (12), 1508–1517. http://dx.doi.org/10.1016/j.envsoft.2010.04.012.

Seligman, N.G., Keulen, H.V., 1981. PAPRAN: a simulation model of annual pasture production limited by rainfall and nitrogen. Conference 192–221.

Shaffer, M.J., 2002. Nitrogen modeling for soil management. J. Soil Water Conserv. 57 (6), 417–425.

Shaffer, M.J., Halvorson, A.D., Pierce, F.J., 1991. Nitrate leaching and economic analysis package (NLEAP): model description and application. Manag. Nitrogen Groundw. Qual. Farm Profitab. 285–322.

Shaffer, M.J., Ma, L., Hansen, S., 2001. Modeling Carbon and Nitrogen Dynamics for Soil Management. CRC Press.

Simek, M., Cooper, J.E., 2002. The influence of soil pH on denitrification: progress towards the understanding of this interaction over the last 50 years. Eur. J. Soil Sci. 53 (3), 345–354. http://dx.doi.org/10.1046/j.1365-2389.2002.00461.x.

Stres, B., Danevčič, T., Pal, L., Fuka, M.M., Resman, L., Leskovec, S., Hacin, J., Stopar, D., Mahne, I., Mandic-Mulec, I., 2008. Influence of temperature and soil water content on bacterial, archaeal and denitrifying microbial communities in drained fen grassland soil microcosms. FEMS Microbiol. Ecol. 66 (1), 110–122.

Tian, H., Chen, G., Lu, C., Xu, X., Ren, W., Zhang, B., Banger, K., Tao, B., Pan, S., Liu, M., Zhang, C., Bruhwiler, L., Wofsy, S., 2015. Global methane and nitrous oxide emissions from terrestrial ecosystems due to multiple environmental changes. Ecosyst. Health Sustain. 1 (1), 1–20. http://dx.doi.org/10.1890/EHS14-0015.1.

Vinten, A.J.A., Castle, K., Arah, J.R.M., 1996. Field evaluation of models of denitrification linked to nitrate leaching for aggregated soil. Eur. J. Soil Sci. 47 (3), 305–317. http://dx.doi.org/10.1111/j.1365-2389.1996.tb01404.x.

Webster, E.A., Hopkins, D.W., 1996. Contributions from different microbial processes to N2O emission from soil under different moisture regimes. Biol. Fertil. Soils 22 (4), 331–335. http://dx.doi.org/10.1007/BF00334578.

Weier, K.L., Doran, J.W., Power, J.F., Walters, D.T., 1993. Denitrification and the dinitrogen nitrous-oxide ratio as affected by soil-water, available carbon, and nitrate. Soil Sci. Soc. Am. J. 57 (1), 66–72. http://dx.doi.org/10.2136/sssaj1993.03615995005700010013x.

Williams, J., 1990. Sharply a N. EPIC-Erosion Productivity Impact Calculator I. Model Documentation, 1768.

Wu, Y., Liu, S., Qiu, L., Sun, Y., 2016. SWAT-DayCent coupler: an integration tool for simultaneous hydro-biogeochemical modeling using SWAT and DayCent. Environ. Model. Softw. 86, 81–90. http://dx.doi.org/10.1016/j.envsoft.2016.09.015.

Zhang, D., Chen, X., Yao, H., James, A., 2016. Moving SWAT model calibration and uncertainty analysis to an enterprise Hadoop-based cloud. Environ. Model. Softw. 84, 140–148. http://dx.doi.org/10.1016/j.envsoft.2016.06.024.